Precipitation enhancement in stratocumulus clouds through airbourne seeding: sensitivity analysis by UCLALES–SALSA

Juha Tonttila[1], Ali Afzalifar[3], Harri Kokkola[1], Tomi Raatikainen[2], Hannele Korhonen[2], and Sami Romakkaniemi[1]

[1]Finnish Meteorological Institute, P.O. Box 1627, 70211, Kuopio, Finland
[2]Finnish Meteorological Institute, P.O. Box 503, 00101, Helsinki, Finland
[3]Aalto University School of Science, Department of Applied Physics, Espoo, Finland

Correspondence: Juha Tonttila (juha.tonttila@fmi.fi)

Abstract. Artificial enhancement of precipitation via hygroscopic cloud seeding is investigated with a numerical large-eddy simulation model coupled with a spectral aerosol-cloud microphysics module. We focus our investigation on marine stratocumulus clouds and evaluate our model results by comparing them with recently published results from field observations. Creating multiple realizations of a single cloud event with the model provides a robust method to detect and attribute the seed-

5   ing effects, which reinforces the analysis based on experimental data. Owing to the detailed representation of aerosol-cloud interactions, our model successfully reproduces the microphysical signatures attributed to the seeding, that were also seen in the observations. Moreover, the model simulations show up to a 2-3 fold increase in the precipitation flux due to the seeding, depending on the seeding rate and injection strategy. However, our simulations suggest that a relatively high seeding particle emission rate is needed for a substantial increase in the precipitation yield, as compared with the estimated seeding concentra-

10   tions from the field campaign. In practical applications, the seeding aerosol is often produced by flare burning. It is speculated, that the required amount of large seeding particles suggested by our results could pose a technical challenge to the flare-based approach.

1   Introduction

Water scarcity is a cause for increasing concern in arid as well as in semi-arid regions (WWAP, 2019). This has revived the

15   interest in research and investments in weather modification efforts, particularly those related to rain enhancement (Flossmann et al., 2019). One of the prominent methods is to purposely introduce large hygroscopic particles into a cloud, which act as cloud condensation nuclei (CCN) and are expected to enhance the growth of droplets and therefore the production of drizzle and precipitation (Bruintjes, 1999; Kuba and Murakami, 2010; Rosenfeld et al., 2010). In spite of numerous experiments on hygroscopic cloud seeding (e.g. Cotton, 1982; Bigg, 1997; Ghate et al., 2007; Jung et al., 2015), estimates of its effect

20   on rainfall are still somewhat uncertain. Given the present consumption rate, the problem of water shortage will most likely become worse, urging for more systematic research efforts to improve the scientific basis for understanding the true effects of seeding with hygroscopic particles.

Attribution of observed effects to artificial perturbations is an intrinsic issue in most field experiments investigating weather modification methods, which makes it difficult to reach a consensus about their applicability. In the case of rain enhancement, it is often problematic to detect the precipitation response to seeding and, in particular, to distinguish it from meteorological variations (Flossmann et al., 2019). Field experiments only provide a single realization of an event: as soon as the cloud is seeded, the reference point is lost, causing it to be very difficult to estimate the unperturbed precipitation rate. This challenges the reproducibility of results from cloud seeding field experiments. Instead, modelling studies provide the advantage of generating multiple realizations of each scenario and, with a carefully planned setup, the experiments are reproducible. Cloud-resolving models comprise an important source of information to complement field campaign studies, as they provide a highly controlled environment for repeatable experiments on the seeding efficacy, which helps to tackle the attribution issue. In this paper, we employ a cloud resolving large-eddy model with sophisticated representation of aerosol-cloud microphysics to study the effects of seeding in marine stratocumulus clouds, which arguably provide the simplest environment where to untangle the governing microphysical processes.

The way in which hygroscopic cloud seeding is expected to influence precipitation is closely related to the effects of naturally occurring giant CCN (GCCN; diameter larger than $1\ \mu$m) and can therefore be considered as being part of the ongoing efforts to understand the aerosol-cloud interactions. In marine boundary layers, GCCN consisting of sea salt is a prominent feature (Jensen and Lee, 2008; Bian et al., 2019). Due to their initial size and the large amount of soluble material, GCCN grow relatively fast in saturated conditions by water condensation and may continue to grow even in a slightly subsaturated environment (Jensen and Nugent, 2017). The presence of GCCN in a cloudy boundary layer has been noted for increasing the mean droplet size and producing higher amounts of precipitation both in experimental (e.g. Lehahn et al., 2011; Dadashazar et al., 2017) and modelling studies (Feingold et al., 1999; Jensen and Lee, 2008; Jensen and Nugent, 2017). The effect of GCCN is caused by two different microphysical mechanisms. First, they suppress the maximum supersaturation during droplet formation due to their water uptake, and thus decrease the total number of cloud droplets. This will yield on average larger droplets and potentially faster precipitation formation. Second, hydrated GCCN increase the width of the cloud droplet size distribution and are thus expected to enhance the collision-coalescence process leading to an increase in precipitation. Additionally, very large wetted GCCN particles may directly contribute to precipitation by acting as raindrop embryos. These processes lay the basic foundation for the hypothesis of hygroscopic cloud seeding to enhance rainfall as well (Kuba and Murakami, 2010; Rosenfeld et al., 2010). The seeding particles, most often delivered to the cloud layer via an aircraft, are typically released by burning flares or from containers with premanufactured milled salt powder (e.g. Jung et al., 2015). It is generally agreed, that the seeding particles need to be in the size range of several micrometers in order to be effective in warm clouds (Segal et al., 2004; Rosenfeld et al., 2010).

In the current work we explore the sensitivity of drizzle and precipitation in marine stratocumulus to hygroscopic cloud seeding using the UCLALES-SALSA (Tonttila et al., 2017) large-eddy model. This modelling package combines the UCLA Large-Eddy Simulation code (UCLALES; Stevens et al., 2005) with the highly detailed microphysical representation by the Sectional Aerosol module for Large-Scale Applications (SALSA; Kokkola et al., 2008). We will investigate the seeding effects in a marine stratocumulus setting based on measurements from a recent field campaign study (Jung et al., 2015). The results

serve the purpose of evaluating the skill of our modelling platform in reproducing the observed microphysical effects as well as to map the importance of the seeding injection strategy and emission rate in terms of the precipitation yield. The remainder of this article continues with the description of the current version of the UCLALES-SALSA model in Section 2. The experimental setup for the model and the specific settings applied in the simulations are summarized in Section 3 followed by description of the results in Section 4. Conclusions are drawn together with some further discussion in Section 5.

2 Model description

UCLALES-SALSA (Tonttila et al., 2017) is built around the well established UCLALES (Stevens et al., 2005) large eddy simulation code, which comprises a modelling platform for idealized cloud simulations. The model uses a 3-dimensional computational mesh with cyclic lateral boundary conditions, including a prognostic description of the three Cartesian wind components. The advection of momentum is based on fourth-order difference equations with time stepping scheme based on the leapfrog method. The prognostic scalar variables include the liquid water potential temperature and variables describing water vapor and condensate amounts, depending on the model configuration. The scalar advection uses a second order flux-limited scheme and the time integration is performed with a simple Eulerian forward time stepping method.

The aerosol and cloud microphysics are represented by the SALSA module. The design of SALSA is described in detail in Kokkola et al. (2008) and Tonttila et al. (2017), but key features are also summarized below, including a description of some important updates. The general layout of the current SALSA module is illustrated in Figure 1. SALSA is a bin microphysics model, describing the size distribution and composition of particles in up to four different categories: aerosol particles, two sets of liquid hydrometeors (cloud droplets and a separate regime dedicated for droplets and precipitation dominated by collision-coalescence growth) and ice (not used in the current work and thus not shown in Figure 1). For aerosol particles and cloud droplets it is possible to use two parallel sets of bins in order to describe externally mixed aerosol populations with separate size distributions.

For particle composition (in all categories), the model uses up to five different aerosol constituents (sulfate, sea salt, organic carbon, black carbon, dust) plus water. Each parameter (particle number and mass of each constituent) in each bin comprises a prognostic scalar variable in UCLALES-SALSA. The model solves all the key microphysical processes for all particle categories, including cloud activation, coagulation and collection processes as well as the condensation of water vapor on both aerosol particles and hydrometeors (see Tonttila et al. (2017) for further details).

The design of SALSA is an attempt 1) to find a compromise between computational cost and model accuracy and, in particular, 2) to be able to track both non-activated and activated particle populations. The latter in particular is fulfilled by setting both the aerosol and cloud droplet bin limits according to the dry aerosol or CCN particle diameter, as illustrated in Figure 1. This allows to preserve the characteristics of the aerosol size distribution at the aerosol – cloud droplet interface. As seen in past model experiments (Tonttila et al., 2017; Boutle et al., 2018), it also provides an adequate description of the droplet size in order to solve the in-cloud microphysical processes. The ability to track the aerosol size distribution in and outside of clouds brings the model a step further from more straight-forward 1-d bin model designs, where information about activated

aerosol is not explicitly tracked. This is also a very important feature for this study, since tracking the evolution of the seeding particles within the cloud is key in order to capture their influence on cloud microphysics and rain formation as well as to analyze and understand the underlying processes.

An important upgrade not described in previous papers concerns the description of precipitation. In the current version, the
95 size distribution for drizzle and rain is described by 20 mass doubling bins (in the wet diameter space) starting from 20 μm. Moreover, instead of a parameterized autoconversion process, we now determine the transition from cloud droplet to drizzle regime directly from the coagulation code. If the droplet diameter resulting from the collision-coalescence between two cloud droplets exceeds the 20 μm limit, the outcome is moved to a drizzle bin with appropriate diameter range. Obviously, the 20 μm limit separating cloud droplets and drizzle is quite small. The decision for this limit was made in favor of more accurate
100 resolution of the droplet size in wet diameter space, where the droplet growth begins to be dominated by collision-coalescence. This helps to ensure a smooth transition from cloud droplets through intermediate sized drizzle (Glienke et al., 2017) to full size drizzle drops and eventually rain. It also provides a more accurate method to describe the growth and transport of GCCN particles within the diameter space, than what was possible with the previously used parameterized autoconversion method (Tonttila et al., 2017).

105 3   Model setup

Marine stratocumulus clouds have been used as the setting for numerous field experiments looking into aerosol-cloud interactions. In a recent study (Jung et al., 2015, henceforward J15), rain enhancement by hygroscopic cloud seeding was investigated from airbourne observations, that took place southwest of Monterey, California, on 3rd August, 2011. We will use this case as the basis for the model experiments in this paper. The meteorological data and aerosol characteristics presented in J15 are used
110 to provide the initial conditions for UCLALES-SALSA. We exploit this setup to investigate the ability of UCLALES-SALSA to simulate the cloud microphysical response to hygroscopic seeding in a series of experiments, consisting of a control run and three cloud seeding runs with different seeding strategies, whose details are outlined below.

3.1   Initial conditions

The measurements reported in J15 took place starting from 16 UTC. We match the model time with this period, which mainly
115 affects the radiative budget at cloud top via the solar zenith angle. The initial profiles of potential temperature and the total water mixing ratio are shown in Figure 2, where the moisture profile is saturated between the levels of approximately 300 m and 650 m. The strength of the potential temperature inversion at the top of the cloud (after condensation of the excess moisture from Figure 2) is approximately 8.5 K. For simplicity, the horizontal wind is initialized to $u = -12$ m s^{-1}, $v = 0$ m s^{-1}, following the standard meteorological notation, which corresponds to the observed wind speed in J15. Surface energy fluxes
120 and the large-scale subsidence are prescribed according to Ackerman et al. (2009) who focus on a similar stratocumulus case. The model grid resolution is set to 50 m (10 m in the vertical) and the domain size is 5 km across laterally, extending up to 1400 m in the vertical. The model timestep is 1 s.

The initial aerosol size distribution is described in the model as a sum of lognormal modes. J15 reported the accumulation mode aerosol concentration in the range of 200 to $800 \, \mathrm{cm^{-3}}$, with CDNC approximately $150 - 200 \, \mathrm{cm^{-3}}$. Therefore, we set

125 the initial accumulation mode concentration to $200 \, \mathrm{cm^{-3}}$. Additional $400 \, \mathrm{cm^{-3}}$ particles were allocated in the Aitken mode, which can be viewed as a typical feature in marine boundary layer (e.g. Zheng et al., 2018). However, for the current setup, the Aitken mode particles reside mostly below the critical size for droplet activation – pilot test runs showed little sensitivity in the results for the Aitken mode number concentration. In addition, natural GCCN particles consisting of sea salt, which are virtually omnipresent in marine boundary layers (Jensen and Nugent, 2017), were assigned to the background aerosol, with

130 mode diameter at $1 \, \mu\mathrm{m}$ and concentration at $1 \, \mathrm{cm^{-3}}$. The lognormal size distribution parameters for the initial model aerosol population are summarized in Table 1.

3.2 Cloud seeding

For the seeding aerosol, we use sea salt as a proxy for the particle composition. We use SALSA's parallel bin regimes to describe the seeding aerosol initially as externally mixed from the background. The seeding aerosol is then allowed to interact

135 with the background particles through coagulation and cloud collection. We will assume two modes for the seeding particles, with mean diameters at $1.5 \, \mu\mathrm{m}$ and $8 \, \mu\mathrm{m}$, which roughly correspond to the mode mean diameters shown in J15, but are also more generally representative of the powdered salt size ranges presumed effective in terms of precipitation enhancement (Rosenfeld et al., 2010).

In the model experiments, the seeding emissions are performed in-cloud, near the cloud top altitude, at approximately 580

140 m, as in J15. Two methods for the release of the seeding particles are considered: i) a domain-wide instantaneous injection of the aerosol at the specified layer and ii) an explicit Lagrangian point source emission. In the former, the particles are assumed to occupy a layer of 50 m in depth. For the latter, the trajectory and speed of the emission source are prescribed. We assume the seeding aerosol plume to immediately occupy a cross-sectional area of $50 \times 50 \, \mathrm{m^2}$. Further dilution of the plume is controlled dominantly by grid-scale mixing. To mimic the airborne emissions, we assume a speed of $60 \, \mathrm{m \, s^{-1}}$ for the source, whose

145 trajectory is illustrated in Figure 3. The seeding source propagates towards the positive x-direction along a trajectory that covers the entire extent of the domain in y-direction. Since the seeding proceeds against the horizontal wind (in x-direction), the seeding is stopped at the middle of the domain. This is to avoid seeding the same plume twice, because the rear of the plume is advected back into the domain from the right due to the cyclic boundary conditions.

Our experimental strategy is to create two parallel sets of realizations: a control simulation without seeding and a set of

150 experiments with seeding particle emissions. This allows to account for both the direct microphysical effects, as well as the dynamical feedbacks potentially caused by the aerosol perturbation. We must take care, that the initial states for the control simulations and sensitivity experiments are identical. Therefore, a "master" model run is performed, from which the model state is saved to a "restart" file prior to the time of the seeding procedure. The length of the "master" run is 4 hours, to allow the boundary-layer mixing and precipitation process to settle in a quasi-steady-state (i.e. spinup). All our model experiments,

155 including both the control and seeding experiments, are initialized from this restart file, which ensures that any differences in the experiments can be attributed directly to the seeding.

The model experiments performed in this study are summarized in Table 2. The seeding experiments Seed1 and Seed2 use the moving point emission source along the trajectory shown in Figure 4. The total seeding rate in the former experiment is set as 1.5×10^{11} s^{-1} and in the latter as 1.5×10^{12} s^{-1}. With the assumed initial plume cross-section and the aircraft speed,

160 this yields an initial plume concentration of approximately 1 cm^{-3} and 10 cm^{-3}, respectively, which will be rather quickly diluted by in-cloud mixing and drizzle formation. In the experiment Seed3 the seeding particles are injected instantaneously in a domain-wide slab at the same altitude as the point emissions in Seed1 and Seed2. The initial concentration in Seed3 is set as 1 cm^{-3}. Comparing the model results between the point source and domain slab emissions and different emission rates helps to understand the impact of the total emitted mass to the efficacy of the seeding, since it critically affects the concentration in

165 the diluted population. Note, that we do not consider the possible aerodynamic effects caused by the aircraft.

3.3 Sensitivity of precipitation

The overall precipitation rate in the simulated case is rather low. The observed estimate reported in J15 is about 0.05 mm h^{-1} on average, sampled around the cloud base height. In order to evaluate the seeding efficacy in UCLALES-SALSA, we want to match the simulated precipitation rate as close as possible to the measurements. We find that in the current case, the precipitation

170 rate is strongly controlled by two key aspects in the model setup: the background aerosol and the vertical resolution. In case of the former, we focus here on the role of natural GCCN, due to their overall small concentration, but potentially strong impact on drizzle formation. For the latter, vertical resolution of the model is known to have a substantial influence on the representation of entrainment mixing at cloud top (Stevens et al., 2005). This is expected to modulate the rate of evaporation of cloud droplets due to the entrained dry air from above the cloud, which affects the mean droplet size and the size distribution

175 width and, therefore, drizzle formation via the collision-coalescence process. Pilot model simulations are performed to test the choices made in our simulation setup.

First, Figure 4 illustrates the effect of GCCN concentration on the simulated precipitation in pilot experiments. With 1 cm^{-3} (used in the experiments), we obtain a precipitation rate much closer to the observed estimate, than with a lower concentration (0.1 cm^{-3}). Similar concentrations of GCCN were also measured in the field campaign according to J15 and the good agree-

180 ment with the observed precipitation rate (0.05 mm h^{-1}) warrants the use of the background aerosol size distribution detailed in Table 1.

Second, Figure 5 shows the effect of vertical resolution on the simulated precipitation rate. It is evident, that 20 m spacing in the model vertical grid yields lower precipitation rate, than the simulations with 5 m or 10 m grid spacings. That said, the difference seen between 5 m and 10 m grid spacings is minor. Even though 10 m resolution has been shown to be inadequate

185 to fully represent the effects of e.g. entrainment mixing, considering this result and the fact that the UCLALES-SALSA is computationally a rather expensive model, we find that the 10 m vertical grid spacing is justified.

4   Results

4.1   Precipitation fluxes

Figure 6 shows the flux of precipitating water sampled at an altitude of 300 m, which is close to the cloud base height. In the
190   control case, the precipitation rate is approximately $0.03 - 0.05 \ \mathrm{mm \ h^{-1}}$, which agrees well with the corresponding measured
precipitation rate in J15. It is evident, that the seeding emission rate and seeding strategy have a strong influence on the
seeding efficiency. The experiment Seed1 (with a low emission rate) yields a positive, but a rather weak signal in terms of the
precipitation flux. Instead, Seed2 (with high emission rate) approximately doubles the precipitation flux within an hour after
the start of the seeding, as compared to the control run. Likewise, even stronger (by a factor of 3) increase in precipitation is
195   shown by Seed3, where the seeding rate is the same as in Seed1, but the total injected mass is much larger because it is applied
to all grid points across the target layer. Therefore, it is important to consider the impact of the seeding strategy on the diluted
plume concentration.

Figure 7 shows the estimated domain mean profiles of the seeding particle concentration. Since the seeding takes place
in-cloud, practically all the particles are activated very quickly. Therefore, the concentration is analysed as the number of
200   cloud droplets formed by the seeding particles, 15 minutes after the seeding. This gives the plumes some time to dilute; with
further delay, the plume concentration starts to be more and more affected by precipitation, after which it is difficult to robustly
distinguish the particles associated with seeding in our modelling setup. Moreover, taking the profile as domain average is
justified because the trajectory of the source in Seed1 and Seed2 is set to cover the entire width of the domain in y direction,
as depicted in Figure 3, and it does not take long for the turbulent diffusion to spread the seeding across the domain area.
205   As indicated in Figure 7, clearly the highest average concentration is seen for Seed3 and the lowest for Seed1, which indeed
emphasizes the connection between the diluted plume concentration to the seeding efficacy. Therefore, as Figure 7 suggests, in
order to produce an approximately 2-fold precipitation yield, the concentration in the diluted plume should be on the order of
$0.01 \ \mathrm{cm^{-3}}$.

4.2   Microphysical signatures

210   The main hypothesized pathways to precipitation enhancement include 1) the reduction of CDNC due to increased competition
for water vapor induced by the large seeding particles and 2) enhanced collision-coalescence (Segal et al., 2004; Rosenfeld et
al., 2010). Thus, to better understand the reasons for the simulated enhanced precipitation shown in Figure 6, we will analyze
more closely the cloud microphysical effects induced by the seeding.

To start with, our model shows very little change in in-cloud relative humidity between the experiments. This is in line
215   with releasing the seeding aerosol close to the cloud top height, following the experimental approach in J15. Consequently,
since most of the ambient aerosol are activated at the level of peak supersaturation close to the cloud base, the water vapor
competition effect appears to be minor in our simulations. However, the simulated cloud droplet number concentration does
show a decrease (Figure 8), which we consider as a sign of enhanced collision-coalescence due to the injection of large CCN

particles. Again, the reduction in CDNC is most pronounced for the highest seeding aerosol emissions, i.e. the experiments

220 Seed2 and Seed3. The strongest reduction is seen in the latter, with a difference by almost 10 % compared to the control case.

More evidence is provided by plotting out the hydrometeor size distributions in the seeding experiments before and after the time of the seeding emission in Figure 9. The size distributions are sampled in-cloud at 300 m altitude, close to the cloud base height. While the size distributions show negligible changes in the experiment Seed1, in Seed2 and Seed3 there is clearly an increase in the concentration of droplets around the 100 μm size range after seeding. After 1 hour, there is also a definite

225 increase in the concentration of larger hydrometeors (> 500 μm), pointing out the time needed for the seeding induced drizzle drops to grow to rain drop sizes by collection processes. In particular, these simulated size distributions, and the effects of seeding therein, bear a remarkable resemblance to the features in the measured size distributions at the corresponding altitude presented by J15; the modelled seeding appears to reproduce the observed effects on the droplet population very closely at the correct size ranges. We consider this to be a very strong argument in support of the ability of UCLALES-SALSA to capture

230 the primary microphysical pathway in how the seeding aerosol affects the precipitation rate.

To close the connection between the microphysical effects and precipitation, Figure 10 shows the contribution to the overall precipitation flux as a function of size. The data in Figure 10 is obtained from the same height level as in Figure 9. As expected, enhanced precipitation due to seeding first takes place by the drizzle size ranges (about 100 μm) and later by the growth of the larger rain drops. The latter is strongly associated with the peak precipitation flux seen just after 5 hours (model time) in Figure

235 6 especially in the experiments Seed3.

5 Discussion and conclusions

The coupled LES-aerosol-cloud model UCLALES-SALSA was used to study the precipitation enhancement by hygroscopic seeding in marine stratocumulus clouds. Results from field observations reported in J15 were used as the basis for a series of model experiments performed to map the dependency of precipitation enhancement on the rate of seeding aerosol emission and

240 the injection strategy. The simulation time period was matched with the observations together with the initial thermodynamic profiles and the ambient aerosol size distributions.

The overall simulated precipitation rates and cloud properties were in good agreement with the results reported in J15, and the simulated mean precipitation flux was approximately $0.03 - 0.05$ mm h^{-1} near the cloud base. Our approach to estimate the effects of seeding was to compare the results between a control run (without seeding) and experiments with seeding, in

245 which the seeding emissions were described both by a moving point emission source and by direct injection of particles to a domain-wide slab. Care was taken to keep the model initial state and the boundary conditions identical between the control run and seeding experiments, so that differences between the simulations could be attributed directly to the seeding aerosol.

Our results show up to 2-3 fold increase in the precipitation flux sampled at cloud base altitude, depending on the experiment. This is comparable to the results in J15. In successful cases, the seeding produces a somewhat sustained effect for up to 2-3

250 hours after the seeding initialization, with the peak enhancement visible within approximately 1-1.5 hours time. However, our results suggest, that the minimum concentration in the seeding particle plume, after allowing it to dilute within the cloud layer,

should be rather high, on the order of 0.01 cm^{-3}, in order to generate an approximately 2-fold precipitation enhancement. This concentration is on the high end of the diluted plume concentrations estimated by J15.

To increase the confidence to our results, the simulated seeding effects on the cloud microphysical properties were inspected.
255 The model simulations skillfully reproduced the seeding effects on the hydrometeor size distribution, as compared with J15. The model size distributions indicated a temporal propagation of increased concentrations first in the drizzle size range and later towards the larger rain drop sizes, which was expected as the result of an enhanced collision growth of droplets. Accordingly, the model also showed a decrease in the total CDNC by up to 10 % due to the seeding emissions. However, again the notable microphysical effects only become visible with the aforementioned 0.01 cm^{-3} diluted seeding plume concentration.
260 In addition, J15 reported a somewhat larger decrease in CDNC after the seeding. Arguably, estimating the seeding efficacy from the model by comparing multiple realizations provides a more robust estimate (at least in terms of the data sampling) than estimating the effects of seeding aerosol from temporally consecutive sets of observations. Given the qualitatively very similar seeding effects between the observations and our model, but a larger decrease in CDNC in the observations than in our model, we speculate that other factors than the seeding alone might be playing a role in the observed cloud layer. These include
265 possible meteorological variations as well as aerodynamic effects from the aircraft used for seeding, which we do not account for in our simulations. The latter has been studied in the context of ice and mixed-phase clouds (Kärcher, 2018; Moisseev et al., 2019), but in terms of warm cloud seeding, a dedicated study would be required.

Flare burning is a commonly used and cost effective method to produce the seeding particles, but they have the tendency to produce particles in a wide range of sizes, with significant contribution from sub-micron particles. Our results highlight the
270 importance of the seeding plume concentrations. Even though the plume concentration can be controlled to an extent both by the emission rate as well as the seeding strategy (e.g. flight plan, use of multiple aircraft), the results corroborate the view presented in recent literature (Rosenfeld et al., 2010), that obtaining a high enough concentration of large ($> 1 \ \mu\text{m}$) CCN from flares in terms of efficient precipitation enhancement might be challenging with currently used practical applications.

Code availability. The model source code is freely available at Github: https://github.com/UCLALES-SALSA/UCLALES-SALSA

275 *Author contributions.* JT and AA share an equal contribution in performing and analysing model experiments, and for writing most of the paper. JT, TR, SR, and H Kokkola are the main contributors in developing the UCLALES-SALSA code. H Korhonen, H Kokkola and SR took part in evaluating the model results and writing the paper.

Competing interests. The authors declare no conflict of interests.

Acknowledgements. This material is based on work supported by the National Center of Meteorology, Abu Dhabi, UAE under the UAE
280   Research Program for Rain Enhancement Science. The work was also supported by the Academy of Finland (project numbers 283031,
309127, 322532, and the Centre of Excellence in Atmospheric Science, 272041) and the European Research Council (project ECLAIR,
646857).

References

Ackerman, A. S., van Zanten, M. C., Stevens, B., Savic-Jovcic, V., Bretherton, C. S., Chlond, A., Golaz, J.-C., Jiang, H., Khairoutdinov, M., Krueger, S. K., Lewellen, D. C., Lock, A., Moeng,C.-H., Nakamura, K., Petters, M. D., Snider, J. R., Weinbrecht, S., and Zulauf, M.: Large-Eddy Simulations of a Drizzling, Stratocumulus-Topped Marine Boundary Layer. Mon. Weather Rev., 137, 1083–1110, doi:10.1175/2008MWR2582.1, 2009.

Bian, H., Froyd, K., Murphy, D. M., Dibb, J., Darmenov, A., Chin, M., Colarco, P. R., da Silva, A., Kucsera, T. L., Schill, G., Yu, H., Bui, P., Dollner, M., Weinzierl, B., Smirnov, A.: Observationally constrained analysis of sea salt aerosol in the marine atmosphere. Atmos. Chem. Phys., 19, 10773-10785, https://doi.org/10.5194/acp-19-10773-2019, 2019.

Bigg, E. K.: An independent evaluation of a South African hygroscopic cloud seeding experiment, 1991-1995. Atmos. Res., 43, 111-127, 1997.

Boutle, I., Price, J., Kudzotsa, I., Kokkola, H., Romakkaniemi, S.: Aerosol–fog interaction and the transition to well-mixed radiation fog, Atmos. Chem. Phys., 18, 7827–7840, https://doi.org/10.5194/acp-18-7827-2018, 2018.

Bruintjes, R.T.: A Review of Cloud Seeding Experiments to Enhance Precipitation and Some New Prospects. Bull. Amer. Meteor. Soc., 80, 805–820, https://doi.org/10.1175/1520-0477(1999)080<0805:AROCSE>2.0.CO;2, 1999.

Cotton, W.R.: Modification of Precipitation from Warm Clouds—A Review. Bull. Amer. Meteor. Soc., 63, 146–160, https://doi.org/10.1175/1520-0477(1982)063<0146:MOPFWC>2.0.CO;2, 1982.

Dadashazar, H., Wang, Z., Crosbie, E., Brunke, M., Zeng, X., Jonsson, H., Woods, R. K., Flagan, R. C., Seinfeld, J. H., Sorooshian, A.: Relationships between giant sea salt particles and clouds inferred from aircraft physicochemical data. J. Geophys. Res. Atmos., 122, 3421–3434, doi:10.1002/ 2016JD026019, 2017.

Feingold, G., Cotton, W. R., Kreidenweis, S. M., Davis, J. T.: the impact of giant cloud condensation nuclei on drizzle formation in stratocumulus: implications for cloud radiative properties. J. Atmos. Sci., 56, 4100–4117, https://doi.org/10.1175/1520-0469(1999)056<4100:TIOGCC>2.0.CO;2, 1999.

Flossmann, A. I., Manton, M., Abshaev, A., Bruintjes, R., Murakami, M., Prabhakaran, T., Yao, Z.: Review of advances in precipitation enhancement research. Bull. Amer. Meteor. Soc., 100, 1465-1480, DOI: 10.1175/BAMS-D-18-0160.1, 2019.

Ghate, V. P., Albrecht, B. A., Kollias, P., Jonsson, H., Breed, D. W.: Cloud seeding as a technique for studying aerosol-cloud interactions in marine stratocumulus. Geophys. Res. Lett., 34, L14807, doi:10.1029/2007GL029748, 2007.

Glienke, S., Kostinski, A., Fugal, J., Shaw, R. A., Borrmann, S., Stith J.: Cloud droplets to drizzle: Contribution of transition drops to microphysical and optical properties of marine stratocumulus clouds. Geophys. Res. Lett., 44, 8002–8010, doi:10.1002/2017GL074430, 2017.

Jensen, J. B., Lee, S.: Giant sea-salt aerosols and warm rain formations in marine stratocumulus. J. Atmos. Sci., 65, 3678-3694, DOI:10.1175/2008JAS2617.1, 2008.

Jensen, J. B., Nugent, A. D.: Condensational growth of drops formed on giant sea-salt aerosol particles. J. Atmos. Sci., 74, 679-697, DOI:10.1175/JAS-D-15-0370.1, 2017.

Jung, E., Albrecht, B. A., Jonsson, H. H., Chen, Y.-C., Seinfeld, J. H., Sorooshian, A., Metcalf, A. R., Song, S., Fang, M., Russell, L. M.: Precipitation effects of giant cloud condensation nuclei artificially introduced into stratocumulus clouds. Atmos. Chem. Phys., 15, 5645-5658, doi:10.5194/acp-15-5645-2015, 2015.

Kokkola, H., Korhonen, H., Lehtinen, K. E. J., Makkonen, R.,Asmi, A., Järvenoja, S., Anttila, T., Partanen, A.-I., Kulmala, M., Järvinen,
320   H., Laaksonen, A., and Kerminen, V.-M.: SALSA – a Sectional Aerosol module for Large Scale Applications. Atmos. Chem. Phys., 8,
2469–2483, doi:10.5194/acp-8-2469-2008, 2008.

Kuba, N., Murakami, M.: Effect of hygroscopic seeding on warm rain clouds – numerical study using a hybrid cloud microphysical model.
Atmos. Chem. Phys., 10, 3335-3351, https://doi.org/10.5194/acp-10-3335-2010, 2010.

Kärcher, B.: Formation and radiative forcing of contrail cirrus. Nat. Commun., 9, 1824, doi:10.1038/s41467-018-04068-0, 2018.

325   Lehahn, Y., Koren, I., Altaratz, O., Kostinski, A. B.: Effect of coarse marine aerosols on stratocumulus clouds. Geophys. Res. Lett., 38,
L20804, doi:10.1029/2011GL048504, 2011.

Moisseev, D., Lautaportti, S., Alku, L.,Tabakova, K., O'Connor, E. J., Leskinen, M., Kulmala, M.: Inadvertent localized intensification of
precipitation by aircraft. J. Geophys. Res. Atmos., 124, 2094–2104, https://doi.org/10.1029/2018JD029449, 2019.

Rosenfeld, D., Axisa, D., Woodley, W. L., Lahav, R.: A quest for effective hygroscopic cloud seeding. J. Appl. Meteor. Climatol., 49,
330   1548–1562, https://doi.org/10.1175/2010JAMC2307.1, 2010.

Segal, Y., Khain, A., Pinsky, M., Rosenfeld, D.: Effects of hygroscopic seeding on raindrop formation as seen from simulations using a
2000-bin spectral cloud parcel model. Atmos. Res., 71, 3-34, doi:10.1016/j.atmosres.2004.03.003, 2004.

Stevens, B., Moeng, C.-H. Ackerman, A. S., Bretherton, C. S., Chlond, A., de Roode, S., Edwards, J., Golaz, J.-C., Jiang, H., Khairoutdi-
nov, M., Kirkpatrick, M. P., Lewellen, D. C., Lock, A., Müller, F., Stevens, D. E., Whelan, E., and Zhu, P.: Evaluation of Large-Eddy
335   Simulations via observations of nocturnal marine stratocumulus. Mon. Weather Rev., 133, 1443–1462, 2005.

Tonttila, J., Maalick, Z., Raatikainen, T., Kokkola, H., Kühn, T., Romakkaniemi, S.: UCLALES–SALSA v1.0: a large-eddy model with
interactive sectional microphysics for aerosol, clouds and precipitation. Geosci. Model Dev., 10, 169–188, https://doi.org/10.5194/gmd-
10-169-2017, 2017.

WWAP (UNESCO World Water Assessment Programme): The United Nations World Water Development Report 2019: Leaving No One
340   Behind. Paris, UNESCO, 2019.

Zheng, G., Wang, Y., Aiken, A. C., Gallo, F., Jensen, M. P., Kollias, P., Kuang, C., Luke, E., Springston, S., Uin, J., Wood, R., Wang, J.:
Marine boundary layer aerosol in the eastern North Atlantic: seasonal variations and key controlling processes. Atmos. Chem. Phys., 18,
17615-17635, https://doi.org/10.5194/acp-18-17615-2018, 2018.

Table 1. Lognormal size distribution parameters for the initial aerosol consisting of three modes (rows). D is the mode mean diameter, N is the mode concentration and σ is the geometric standard deviation.

D[μm]	N[cm^{-3}]	σ
0.022	400	1.2
0.12	200	1.7
1	1	1.7

Table 2. List of model experiments, including the seeding particle injection method and the lognormal size distribution parameters for seeding. Subscripts 1 and 2 refer to the two lognormal modes used for the seeding aerosol. D is the mode mean diameter, N is the mode concentration and σ is the geometric standard deviation.

Experiment	Seeding strategy	$D_1[\mu m]$	$N_1[cm^{-3}]$	σ_1	$D_2[\mu m]$	$N_2[cm^{-3}]$	σ_2
CTRL	N/A	-	-	-	-	-	-
Seed1	Point source	1.6	0.5	1.3	8	0.5	1.6
Seed2	Point source	1.6	5	1.3	8	5	1.6
Seed3	Full slab	1.6	0.5	1.3	8	0.5	1.6
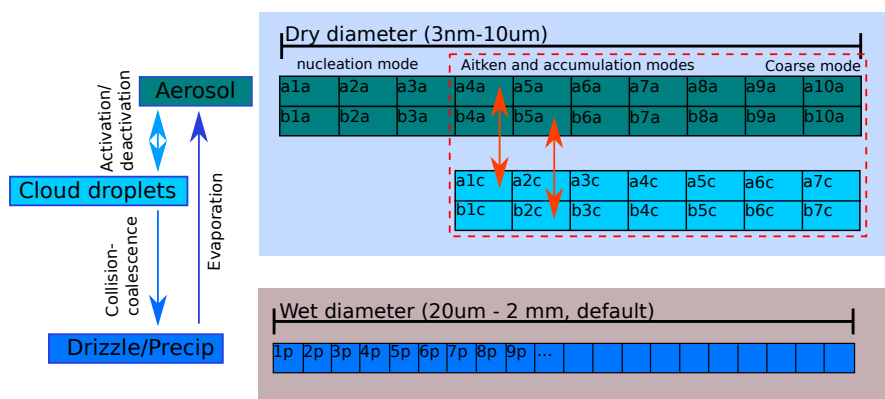
Figure 1. Schematic illustration of the microphysical interactions between the binned size distributions of different particles categories implemented in SALSA.
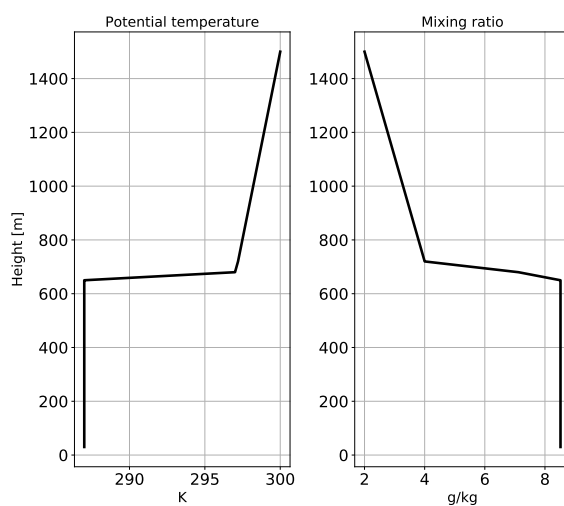
Figure 2. Input profiles of potential temperature and total water mixing ratio. The layer from approximately 300 m to 650m is saturated.
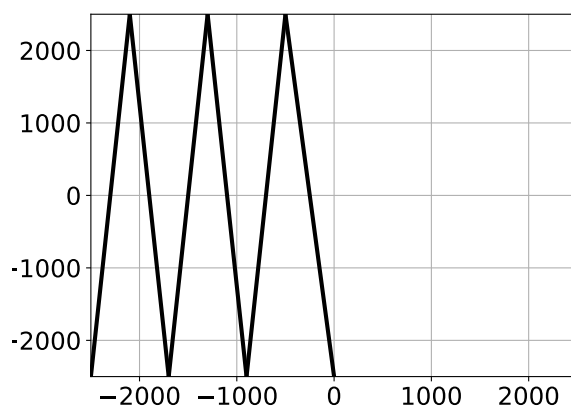
Figure 3. Trajectory of the cloud seeding emissions source on an x-y plane. The seeding starts from the lower left corner and progresses along the black line towards the positive x-direction.
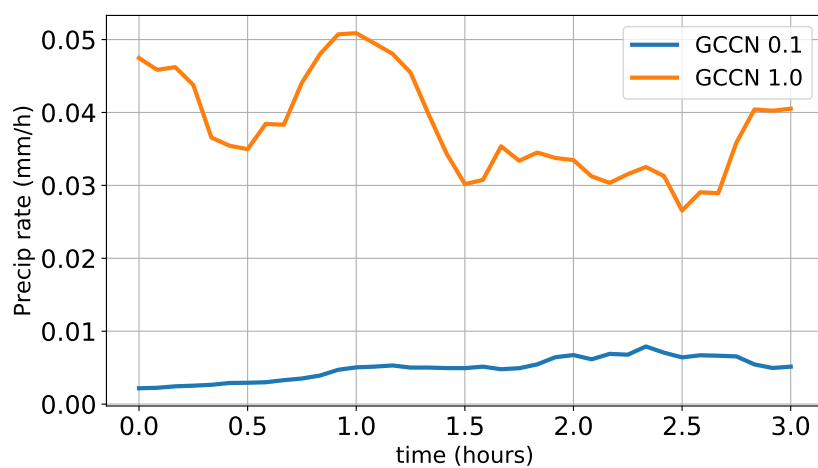
Figure 4. Effect of GCCN on precipitation rate close to cloud base (300 m). Precipitation rate is shown for low ($0.1\ \mathrm{cm}^{-3}$; blue) and high ($1.0\ \mathrm{cm}^{-3}$; orange) GCCN concentrations as a function of time.
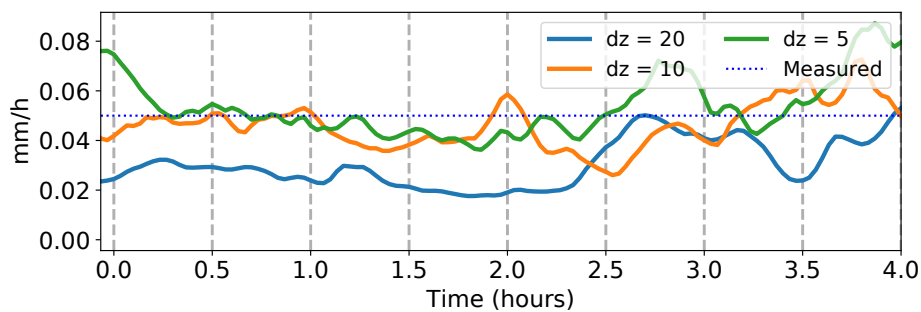
Figure 5. Effect of vertical resolution on the mean precipitation flux close to cloud base (300 m) as a function of time. The dashed blue line shows the corresponding precipitation rate estimated in J15.
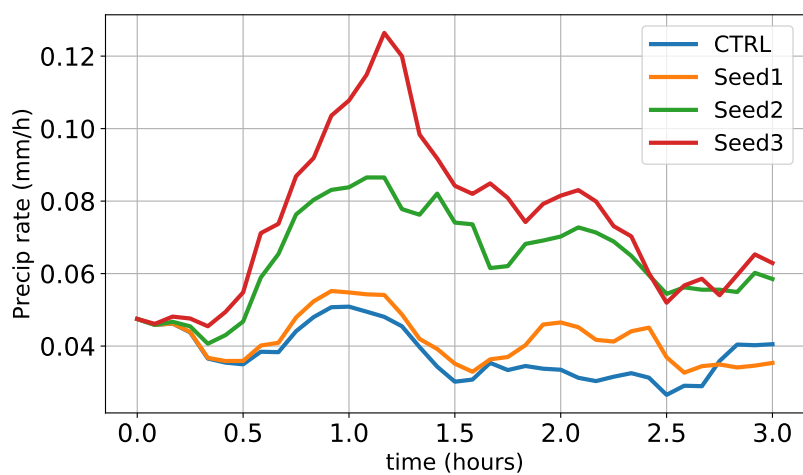
Figure 6. Domain mean precipitation rate at cloud base as a function of time in the control run and the seeding experiments. 0 hours time marks the start of the seeding emission.
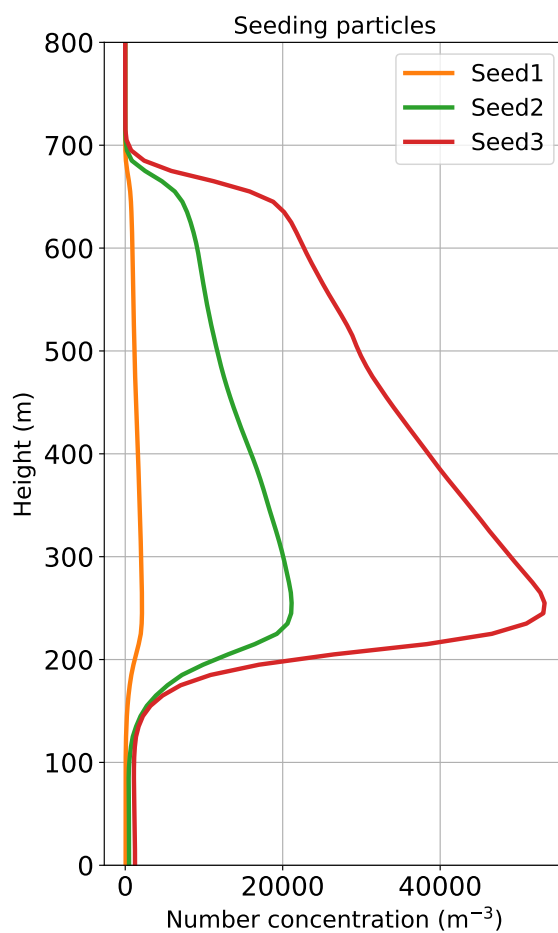
Figure 7. Domain mean profile of seeding particle concentrations 15 minutes after their release in the seeding experiments.
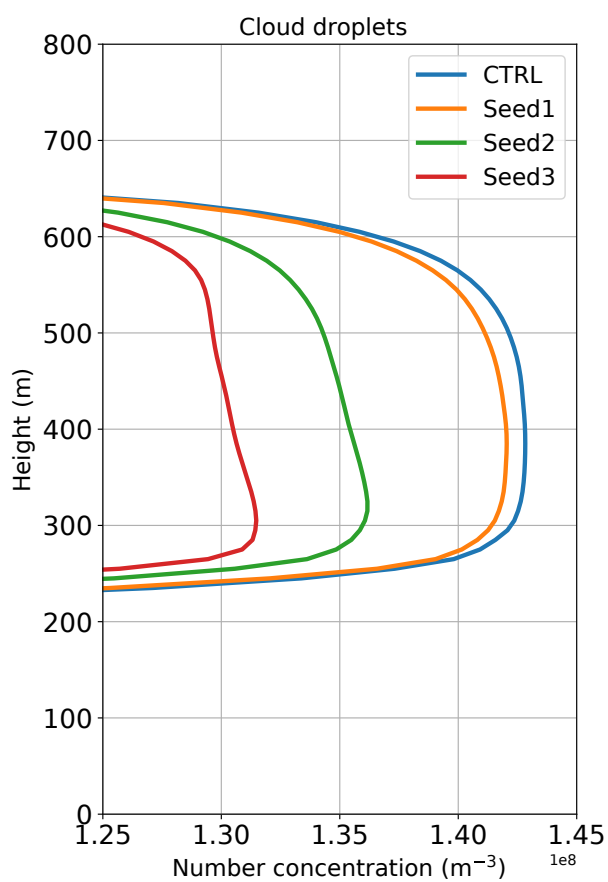
Figure 8. Domain mean cloud droplet number concentration 1 hour after the seeding time in the control run and the seeding experiments.
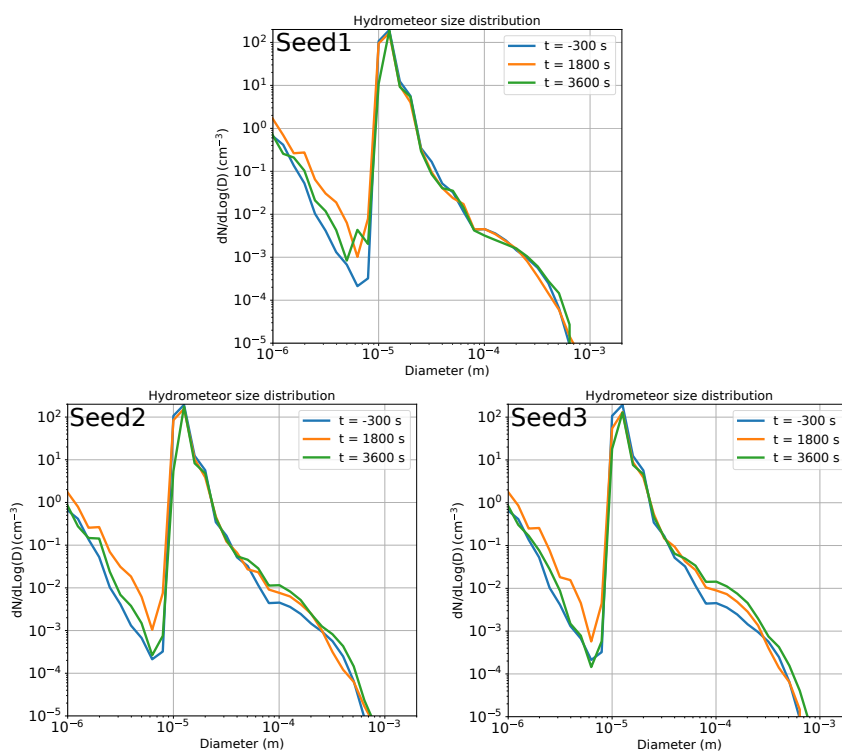
Figure 9. Hydrometeor size distributions close to cloud base (300 m altitude) before (-300 s) and after (1800 s and 3600 s) the particle injection in the seeding experiments.
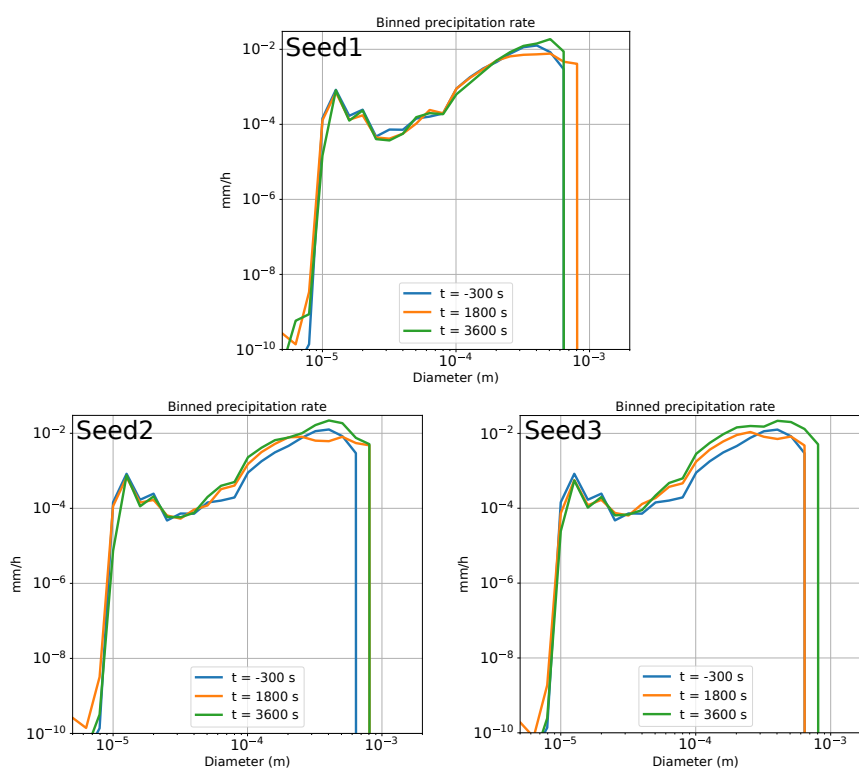
Figure 10. The contribution of hydrometeors to the total precipitation rate at cloud base as a function of size before (-300 s) and after (1800 s and 3600 s) the particle injection in the seeding experiments.